

## NeuLAND - from prototypes to double-planes\*

K. Boretzky<sup>†1</sup>, B. Agrawal<sup>3</sup>, G.D. Alkhazov<sup>11</sup>, S. Altstadt<sup>9</sup>, H. Alvarez Pol<sup>17</sup>, V.A. Andreev<sup>11</sup>, L. Atar<sup>2</sup>, T. Aumann<sup>2,1</sup>, V. Babić<sup>13</sup>, P. Basu<sup>3</sup>, D. Bemmerer<sup>4</sup>, M. Bendel<sup>14</sup>, D. Bertini<sup>1</sup>, P. Bhattacharya<sup>3</sup>, S. Bhattacharya<sup>3</sup>, A. Blanco<sup>5</sup>, J. Bonilla<sup>9</sup>, C. Caesar<sup>2</sup>, L. Cartegni<sup>7</sup>, S. Chakraborty<sup>3</sup>, A. Charpy<sup>13</sup>, S. Chatterjee<sup>3</sup>, M. Cherciu<sup>6</sup>, L. Chulkov<sup>12</sup>, M. Ciobanu<sup>6</sup>, T. Cowan<sup>4,10</sup>, U. Datta Pramanik<sup>3</sup>, G. Dentinger<sup>2</sup>, Z. Elekes<sup>18</sup>, A.A. Fetisov<sup>11</sup>, E. Fiori<sup>15</sup>, P. Fonte<sup>5</sup>, D. Galaviz<sup>7</sup>, I. Gašparić<sup>19</sup>, J. Gerbig<sup>9</sup>, R. Gernhäuser<sup>14</sup>, K. Göbel<sup>9</sup>, V.L. Golotsov<sup>11</sup>, M. Haiduc<sup>6</sup>, T. Heftrich<sup>9</sup>, J. Hehner<sup>1</sup>, M. Heil<sup>1</sup>, M. Heine<sup>2</sup>, A. Heinz<sup>13</sup>, A. Henriques<sup>7</sup>, M. Holl<sup>2</sup>, A. Ignatov<sup>2</sup>, G. Ickert<sup>1</sup>, J. Isaak<sup>15</sup>, E.A. Ivanov<sup>11</sup>, S. Jährling<sup>2</sup>, J. Johansen<sup>2</sup>, H. Johansson<sup>13</sup>, J. Kahlbow<sup>2</sup>, A. Kelić-Heil<sup>1</sup>, O. Kiselev<sup>1</sup>, R. Kissel<sup>2</sup>, K. Kobayashi<sup>20</sup>, D. Körper<sup>1</sup>, D. Kresan<sup>2</sup>, A.G. Krivshich<sup>11</sup>, P. Kumar Das<sup>3</sup>, T. LeBlais<sup>14</sup>, C. Lederer<sup>9</sup>, Y. Leifels<sup>1</sup>, S. Lindberg<sup>13</sup>, L. Lopes<sup>5</sup>, B. Löher<sup>15</sup>, J. Machado<sup>7</sup>, J. Marganiec<sup>2</sup>, L. Netterdon<sup>8</sup>, T. Nilsson<sup>13</sup>, V. Panin<sup>2</sup>, J. Panja<sup>3</sup>, S. Paschalis<sup>2</sup>, A. Perea<sup>16</sup>, S.G. Pickstone<sup>8</sup>, B. Pietras<sup>17</sup>, R. Plag<sup>1</sup>, M. Pohl<sup>9</sup>, M. Potlog<sup>6</sup>, A. Rahaman<sup>3</sup>, G. Rastrepina<sup>9</sup>, A. Ray<sup>3</sup>, R. Reifarth<sup>9</sup>, T. Reinhardt<sup>10</sup>, G. Ribeiro<sup>16</sup>, M. Röder<sup>10</sup>, D. Rossi<sup>1</sup>, J. Sánchez del Río<sup>16</sup>, A. Sauerwein<sup>9</sup>, D. Savran<sup>15</sup>, H. Scheit<sup>2</sup>, F. Schindler<sup>2</sup>, S. Schmidt<sup>9</sup>, P. Schrock<sup>2</sup>, J. Silva<sup>15</sup>, H. Simon<sup>1</sup>, T. Sinha<sup>3</sup>, M. Sobiella<sup>4</sup>, K. Sonnabend<sup>9</sup>, D. Stach<sup>4</sup>, E. Stan<sup>6</sup>, O. Tengblad<sup>16</sup>, P. Teubig<sup>7</sup>, R. Thies<sup>13</sup>, L.N. Uvarov<sup>11</sup>, P. Velho<sup>7</sup>, V.V. Vikhrov<sup>11</sup>, S.S. Volkov<sup>11</sup>, V. Volkov<sup>2,12</sup>, A. Wagner<sup>4</sup>, F. Wamers<sup>2</sup>, M. Weigand<sup>9</sup>, M. Winkel<sup>14</sup>, J. Wüstenfeld<sup>4</sup>, D. Yakorev<sup>4</sup>, A.A. Zhdanov<sup>11</sup>, A. Zilges<sup>8</sup>, K. Zuber<sup>10</sup>, for the R<sup>3</sup>B collaboration, and the FAIR@GSI RBRB<sup>1</sup>

<sup>1</sup>GSI, Darmstadt, Germany; <sup>2</sup>TU Darmstadt, Germany; <sup>3</sup>SINP Kolkata, India; <sup>4</sup>HZDR, Dresden-Rossendorf, Germany; <sup>5</sup>LIP, Coimbra, Portugal; <sup>6</sup>ISS, Bucharest, Romania; <sup>7</sup>Univ. Lisbon, Portugal; <sup>8</sup>Univ. of Cologne, Germany; <sup>9</sup>Univ. Frankfurt, Germany; <sup>10</sup>TU Dresden, Germany; <sup>11</sup>PNPI St. Petersburg, Russia; <sup>12</sup>Kurchatow Institute Moscow, Russia; <sup>13</sup>Chalmers Univ. of Technology, Göteborg, Sweden; <sup>14</sup>TU München, Germany; <sup>15</sup>EMMI, GSI Darmstadt, Germany; <sup>16</sup>CSIC Madrid, Spain; <sup>17</sup>U Santiago de Compostela, Spain; <sup>18</sup>MTA ATOMKI, Debrecen, Ungarn; <sup>19</sup>RBI, Zagreb, Croatia; <sup>20</sup>Rikkyo University, Tokyo, Japan

### Overview

During 2013 the NeuLAND (new Large-Area Neutron Detector) project passed the important step from prototype tests to series production. Being one of the key instruments of the R<sup>3</sup>B experiment [1] the NeuLAND demonstrator will be utilized in the 2014 beam times together with demonstrators of other major R<sup>3</sup>B components.

NeuLAND is a highly granular detector composed of 3000 scintillator bars with a total volume of 250x250x300 cm<sup>3</sup>. It enables the detection of fast neutrons with high efficiency, high time and spatial resolution and a high resolving power for multi-neutron events [2].

Despite the compact cubical arrangement of the NeuLAND components, the detector is built up from individual subgroups with an independent functionality, the so-called NeuLAND *double-planes*. This modular design facilitates maintenance and it allows upon experimental needs to split the detector in subdetectors being located at different positions with respect to the target area.

\* Work supported by FAIR@GSI PSP code 1.2.5.1.2.5., by BMBF (06DA70471, 06FY71051, 06KY71593,06DR1341, NupNET NEDEN-SAA 05P09CRFN5), by ENSAR, by GSI via the GSI-TU Darmstadt co-operation contract, by GSI F&E (DR-ZUBE) and by HIC for FAIR.

<sup>†</sup> k.boretzky@gsi.de

### NeuLAND Double-Planes

During the previous year the first three double-planes of NeuLAND have been built. Here, we report about its different building blocks, the assembly into the double-plane structure and into the demonstrator frame. A double-plane is built up from 100 scintillator bars, 50 forming a vertical / horizontal oriented plane each. 200 photomultipliers (PMTs) serve to read out the scintillator bars from both far ends and consequently 200 channels of high voltage supply (HV) and read out electronics are required for each double-plane.

#### Scintillator Bars

The heart pieces of NeuLAND are the fully-active scintillator bars from BC408-equivalent with dimensions 250x5x5 cm<sup>3</sup> of rectangular shape. To avoid light losses at transitions between different materials, the bars are produced in one piece with its light guides at the two far ends. The light guides of conical shape are 10 cm long and connect the quadratical surface with a one-inch circular surface, thus leading to a total bar length of 270 cm. Within a frame contract concluded in 2013 the scintillator bars can be ordered in several fractions to fixed conditions over a period of four years. Within the first order 430 bars have been purchased allowing together with the prior existing

200 bars to built up six double-planes, thus a 20% NeuLAND demonstrator. The scintillator bars are delivered with reflective and with light-tight wrapping.

Prior to their assembly into double-planes the bars undergo a site acceptance test, controlling both the quality of the scintillator material itself and the surface finishing. The test procedure developed and carried out by the contributing NeuLAND collaborators comprises a measurement of the response to cosmic rays and a measurement of the light transport using a light emitting diode (LED) shining in at one far side of the scintillator bar and being detected at the opposite side. The resulting data are compared to the results for a quality-proven reference bar. Figure 1 shows a typical QDC spectrum from such a combined cosmic and LED test.

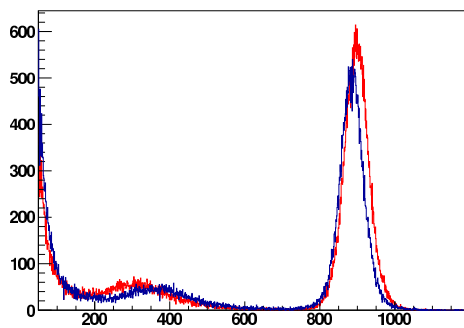


Figure 1: QDC spectra (counts vs. channel number) taken for the reference bar (red) and bar 29 (blue) of 2013 delivery. The prominent peak at about channel number 900 originates from the LED pulse, while the broad peak at channel number  $\approx 300$  stems from cosmic rays traversing the bar.

### Photomultiplier

For the light read out from the scintillator bars one-inch PMTs are connected to the far ends of the scintillator bars. The selected NeuLAND PMT R8619-20 comprises high-quality performance with cost-effectiveness; a fully active voltage divider has been developed for the use in NeuLAND in order to minimize the current demands. For the PMTs, as for the scintillator bars, a frame contract allows the fractional purchase at fixed conditions within the next four years. In the first order, PMTs to assemble the 20% demonstrator have been purchased.

The light-coupling between scintillator bar and PMT front face was subject to investigations taking into account not only the maximization of light read out, but also the long term sustainability and the possibility to apply the coupling material to vertically and horizontally oriented PMTs. A coupling via silicon glue was selected after curing issues had been successfully minimized.

### High Voltage Supply

The high voltage supply for the NeuLAND PMTs is supposed to be unitized in a manner, that each double plane is equipped with its own high voltage distribution system close by, thus enabling the modular operation of NeuLAND double planes. The final layout of the high voltage system is under investigation at the moment. During the 2014 beam times the NeuLAND demonstrator will be brought into operation using commercial high voltage supplies available from other GSI detector systems.

### Read-Out Electronics

The current concept for the read-out electronics is based on a concept originally developed within the FOPI collaboration, the so-called Tacquila readout system. The system provides a fully integrated solution of both charge and time measurement behind a dedicated frontend-card which is used to condition and split the signals. Here, one part is directly connected to a QDC board, while the other is put through an discriminator and further provided to the time measurement using an ASIC based solution. A dedicated frontend has been developed and commissioned in the last years, using the LAND detector, providing an optimized signal treatment for photomultiplier signals. The frontend cards are controlled using the TRIPLEX card [3] which is also used to provide monitoring access to each channel in the electronics. Currently a new electronic readout system, based on the FEBEX readout architecture utilizing an FPGA TDC [4] called Tamex has been designed, and first prototypes are currently being built. The system makes use of the previously done developments, as it is compatible to the existing analog frontend, discriminator and controls environment, by reusing the already existing cards design. The digital backend does not rely any longer on the out phased ASIC and is furthermore multi-hit capable, as well it provides time-over-threshold information. All double planes as shown in figure 3 will such be equipped with their individual readout electronics for 200 channels, and can be operated in a self-sustained manner, making best use of a fully modular design.

### NeuLAND frames

A dedicated frame structure was designed to assemble the scintillator bars and PMTs into double-planes. Fig. 2 shows from left to right an empty double-plane frame, a frame with half of the bars mounted and a fully equipped double-plane frame. Each bar is separately mounted to the frame using a block holding structure, which fits to the conical endings of the bars. In order to protect the horizontal bars from bending in the middle, each bar is supported twice using a metal band structure with individual segments for each bar (visible on the photograph in the middle of fig. 2).

The PMTs are mounted to the bars via guide tubes from stainless steel. A light-tight connection to the holding



Figure 2: The Photographs show (left to right) an empty double-plane frame, a frame after mounting of the vertically oriented bars and after installation of the support structure for the horizontally oriented bars and a frame after assembly of all scintillator bars prior to mounting of PMTs.

blocks is provided using O-rings. The far end of the guide tube is closed with an endcap containing a bajonet lock allowing an easy access to the PMT for maintenance. The signal and HV-cables are fed through an elastomer cap for light-tightness.

The signal and HV cable of the PMTs are connected to collector boards mounted along the read-out sides of the frame. Connections to these boards are provided via LEMO and CLIFF contacts, again allowing for an easy exchange of PMTs in case of maintenance. From the boards the cabling to HV distribution and to the readout electronic is provided via multipin connectors.

### Assembly of NeuLAND substructures

A NeuLAND rack with two-fold purpose was built, see fig. 3. It serves for assembly of the NeuLAND double-planes and it allows to host up to six double-planes, thus the NeuLAND demonstrator.

The assembly, cabling and the commissioning of the NeuLAND double-planes is carried out by the funding collaborators.

### Results from the Experiment S406

In November 2012 150 scintillator bars in a special configuration with 15 layers of ten vertical bars each were exposed to monoenergetic fast neutrons stemming from deuteron breakup reactions in a  $\text{CH}_2$  target, see last year's report for details [5]. Here we report about the status of the analysis of the collected neutron data and its implications on the NeuLAND simulation algorithms.

The calibration of the NeuLAND data taken in this experiment (S406) is completed. Apart from the usual calibration steps special care has been taken of the walk correction of the NeuLAND Tacquila channels. It improved the earlier reported value of time resolution for deuteron beam from  $\sigma_t^D = 115$  ps to 96 ps. The data collected allow a detailed study of hit patterns of neutron-induced particle tracks. A top view of one event with a neutron interaction in the first plane is illustrated in fig. 4. One digit in the histogram corresponds to one bar. The neutron impinges from



Figure 3: Photograph of the NeuLAND mounting and demonstrator rack together with the first NeuLAND double-plane.

the left side. A high-energetic secondary particle is produced, which propagates through the detector (total depth of 0.75 m), indicated by the strict time order of the detected signals (z-axis).

The analysed neutron data in the NeuLAND test array is used to optimize the simulations. At this stage of the data analysis the neutrons are accepted as valid hits if a proper time correlation to the beam velocity is found. This might include besides reactions on the hydrogen also reactions on the carbon in the  $\text{CH}_2$  target and breakup in the close-by start detector. As the next step the analysis of quasi-free scattered (QFS) protons in Crystal Ball and Silicon Strip Detectors is performed. The typical signa-

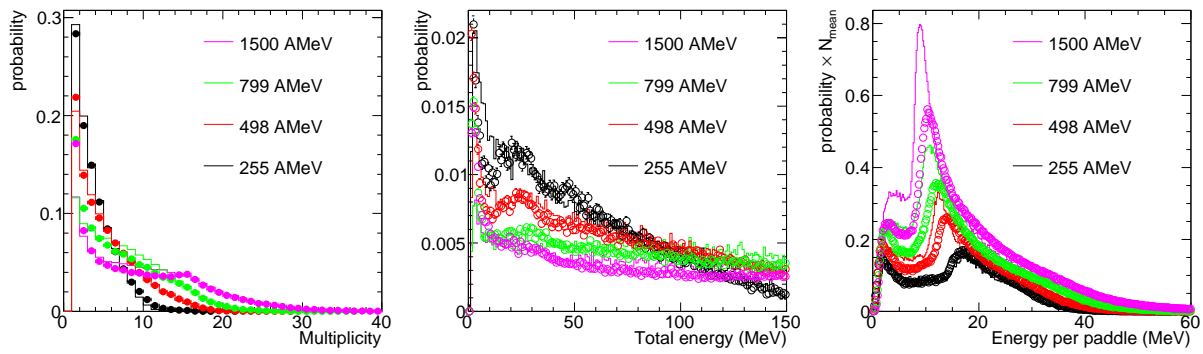


Figure 5: Probability distributions for neutrons of various energies from experimental data (symbols) and corresponding simulation (lines). Displayed in the left-hand panel is the hit multiplicity per incident neutron. The middle panel shows the total deposited energy in the NeuLAND test array per neutron and the right-hand panel the energy deposited per scintillator bar. For the latter the probability was multiplied with the average number of hits  $N_{mean}$  for each neutron energy.

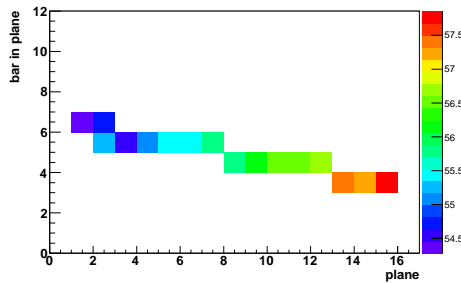


Figure 4: Display of one neutron-induced charged particle track traversing the NeuLAND test array. The time in ns is indicated on the z-axis.

tures for QFS events are observed in correlations of polar and azimuthal proton angles. The further analysis oriented to elimination of the background and the reconstruction of the neutron kinematics is underway.

In the NeuLAND simulation and reconstruction algorithm for experiment S406 neutrons, which are emitted from ppn reactions of deuteron with hydrogen in the target, are transported through the modelled experimental setup by calculating their interaction with scintillator bars using a step-wise Monte-Carlo simulation engine Geant3. During this step of simulation, the energy loss of induced charged particles is converted into light equivalent, also applying light quenching for protons. The output represents the so-called Monte Carlo Points, which describe the energy loss of one charged particle per one scintillator bar. Thus, a sophisticated hit producer (digitizer) algorithm is required, described below, in order to match with the real data from experiment.

On the single particle level, the light attenuation is taken into account according to the position of deposited energy in the detector and the time resolution is applied using a

Gaussian smearing with  $\sigma = 150$  ps. The general start time value for the charge integration is determined and the energy loss of all particles in each bar is integrated, applying position dependent time decay of the signal. As a next step the hits (digis) in the detector units are treated. The saturation of a single PMT is taken into account as well as the resolution of the QDC (smearing the calculated charge with a Gaussian of  $\sigma = 3 - 4\%$ ) and the individual PMT thresholds using the values obtained from data analysis. The PMT saturation formula used here  $QDC_{out} = QDC_{in} * 1. / (1. + 0.012 * QDC_{in})$  is in agreement with laboratory tests of the NeuLAND PMT with LED light.

Various quantities are regarded to compare experimental results to simulations, see fig. 5. In the right hand panel the measured probability distribution of the hit multiplicity per incident neutron is compared to the simulated one for neutron energies ranging from 200 to 1500 MeV<sup>1</sup>. As expected the hit multiplicity increases with increasing neutron energy.

The probability distribution of the total deposited energy is displayed in the middle panel and the energy deposited per scintillator bar in the right-hand panel. It turned out, that two effects play a mayor role for the description of the data within the simulation. The individual realistic thresholds from the experiment are crucial for the comparison of multiplicity spectra and the low energy part of the energy spectra. The proper treatment of the PMT saturation is necessary for understanding higher energy deposition in a single bar and for the total energy deposition in the NeuLAND test array. The slight discrepancies at lower deposited energies may origin from differences in the PMT saturation due to different exposure to magnetic fields for the different beam energies and from background effects in the experiment not yet taken into account.

<sup>1</sup>The experimental data for 200 MeV are compared to simulation findings for 250 MeV, since the quasi free event generator was available for the slightly higher beam energy solely.



Overall a good agreement between data and simulation is found over this very large range of incident neutron energies with one consistent description of the physics processes in the R<sup>3</sup>Broot simulation. This improvement in the description is a very valuable basis for the ongoing further development of algorithms for the final NeuLAND detector.

### Perspectives

In spring and summer 2014 beam times take place at Cave C at GSI in order to commission demonstrators of various R<sup>3</sup>B detectors. The first NeuLAND double-plane will be tested during the April beam time, for summer the commissioning of four to six double-planes (20% demonstrator) is scheduled. Due to the lack of beam time availability during 2015 at GSI, the further commissioning and use of several NeuLAND double-planes at RIKEN are planned.

### References

- [1] A next generation experimental setup for studies of Reactions with Relativistic Radioactive Beams, <https://www.gsi.de/work/forschung/nustarennakernreaktionen/activities/r3b.htm>
- [2] NeuLAND@R3B: A Fully-Active Detector for Time-of-Flight and Calorimetry of Fast Neutrons, NeuLAND Technical Design Report, <http://www.fair-center.de/fileadmin/fair/experiments/NUSTAR/Pdf/TDRs/NeuLAND-TDR-Web.pdf>
- [3] TRIPLEX, an Upgrade for the TACQUILA System, K. Koch et al, GSI Sci. Rep. 2010, PHN-IS-EE-07, p. 235.  
Heading towards FAIR: upgrades on the R3B-Cave C electronics, C. Cäsar et al, GSI Sci. Rep. 2009, INSTRUMENTS-METHODS-30, p. 310.
- [4] Field-Programmable-Gate-Array Based Signal Discrimination and Time Digitisation, C. Ugur et al., GSI Sci Rep 2012, PHN-SIS18-ACC-43 FAIR@GSI, p.299.  
Design and implementation of a data transfer protocol via optical fibre, S. Minami et al., GSI SCIENTIFIC REPORT 2009, INSTRUMENTS-METHODS-51, p.331.
- [5] K. Boretzky et al., Construction and Test of a Large NeuLAND Prototype Array, GSI Scientific Report 2012, <http://repository.gsi.de/record/52093/files/PHN-ENNA-EXP-60.pdf>
- [6] D. Kresan et al., Recent Developments in NeuLAND, GSI Scientific Report 2012, <http://repository.gsi.de/record/52097/files/PHN-ENNA-EXP-64.pdf>